JOURNAL OF DEGRADED AND MINING LANDS MANAGEMENT
Volume 9, Number 4 (July 2022):3763-3772, doi:10.15243/jdmlm.2022.094.3763
ISSN: 2339-076X (p); 2502-2458 (e), www.jdmlm.ub.ac.id

Research Article

Changes in peak discharge based on sago land use scenarios in the upstream Rongkong watershed, Indonesia

Yumna[1*], Sugeng Prijono[2], Wahid[1], Srida Mitra Ayu[1], Witno[1]

[1] Faculty of Forestry, Andi Djemma University, Jl. Puang H. Daud No. 4, Palopo, Indonesia
[2] Department of Soil Science, Faculty of Agriculture, Jl. Veteran No. 1 Malang 65145, Indonesia

[*]corresponding author: yumnaunanda588@gmail.com

Article history:
Received 6 May 2022
Accepted 11 June 2022
Published 1 July 2022

Keywords:
flooding
land cover
runoff
sago palm
watershed

Abstract

Land use affects changes in peak discharge so that it has the potential to cause or prevent flooding. Sago has morphological characteristics that have the potential to absorb more water. This study aimed to determine the magnitude of the change in peak discharge in the upstream watershed after sago planting. Observations were made on the three growth phases of sago palms (initial, middle, and mature phases). The research stages included calculating the runoff coefficient value under sago stands at three growth phases. Peak discharge of the existing conditions (settlements, rice fields, mixed gardens, shrubs, sand dunes, forests, and water bodies) was estimated after three scenarios of sago land use. The scenarios consisted of 25% of the land area planted with sago (scenario 1), 50% for scenario 2, and 100% for scenario 3. The data were analyzed quantitatively by comparing peak discharge in the existing conditions with scenario results. The results showed that the peak discharge in the existing conditions was 52.36 m^3 $hour^{-1}$. Peak discharge in the initial phase of scenario 1 was 18.94 m^3 $hour^{-1}$, scenario 2 was 37.88 m^3 $hour^{-1}$, and scenario 3 was 75.77 m^3 $hour^{-1}$. Peak discharge in the middle phase of scenario 1 was 19.01 m^3 $hour^{-1}$, scenario 2 was 38.02 m^3 $hour^{-1}$, and scenario 3 was 76.04 m^3 $hour^{-1}$. Peak discharge in the mature phase of scenario 1 was 6.38 m^3 hour, scenario 2 was 12.76 m^3 $hour^{-1}$, and scenario 3 was 26.55 m^3 $hour^{-1}$. The peak discharge in the upstream watershed decreased after the scenarios with the use of sago land for all growth phases, except for scenario 3 of the initial and middle phases.

To cite this article: Yumna, Prijono, S., Wahid, Ayu, S.M. and Witno. 2022. Changes in peak discharge based on sago land use scenarios in the upstream Rongkong watershed, Indonesia. Journal of Degraded and Mining Lands Management 9(4):3763-3772, doi:10.15243/jdmlm.2022.094.3763.

Introduction

The Rongkong watershed is one of the priority watersheds in eastern Indonesia. The priority of handling the Rongkong watershed is caused by flooding events that occur periodically every decade. The hydrological conditions of the last five years are getting worse where flood events occur every year, even several times a year. The biggest flood event occurred in 2019, which devastated North Luwu Regency, South Sulawesi. The loss of life and material casualties is very large, and the trans Sulawesi transportation route was cut off. Some facts about the Rongkong watershed that cause flooding include very high rainfall (>3,900 mm per year) and no season zone (rain throughout the year). Factors causing flooding in the Rongkong watershed are high rainfall and very steep topography that cannot be controlled. Rainwater products will mostly become surface runoff (de Almeida et al., 2021) and then flow into rivers and, within a certain time, will overflow into floods in the middle and downstream parts (Asitatikie et al., 2021; Sonu and Bhagyanathan, 2022). In addition to climatological factors, there are also land morphological factors, which are about 70% of the

Rongkong watershed area; the topography is steep to very steep. About 30% of the land is lowland with an altitude of 0 to 3 meters above sea level. Settlements spread to extreme topographic conditions, as well as land use patterns that still do not pay attention to conservation rules (Yumna et al., 2019). Human activities in land use that are not in accordance with conservation principles can change the function of land to absorb and store water in the soil (Aburas et al., 2019; Assefa et al., 2020). This condition will be exacerbated if climatological factors, especially high rainfall (Ridwan et al., 2021), interact with steep to very steep landscapes (Ao et al., 2021; Ma et al., 2021). Many studies have been carried out on flood control through vegetation restoration (Mu et al., 2019; Zheng et al., 2021). Xu et al. (2018) and Sun et al. (2021) showed that vegetation restoration had not shown maximum results in reducing runoff. However, the vegetation used is typical in each area with different characteristics. Therefore, a wise approach that can be considered is to pay attention to land use patterns. The pattern of land use in question includes the accuracy of choosing plant types that have important values from the socio-economic aspect but do not ignore the ecological aspect. One type that meets these rules is the sago palm.

The public perception of the sago palm is that they assume that sago is a lowland plant that only grows and produces well on land that is always flooded and does not require management. However, Yumna et al. (2020) reported that sago palms could grow ideally of plants grown on land at an altitude above 700 m above sea level. Even the quality and quantity of sago starch produced are high if sago plants are grown on dry land (Ming et al., 2018; Yater et al., 2019). Yumna et al. (2029) reported that based on land suitability analysis, the upland upstream of the Rongkong watershed is suitable and very suitable for sago plants. The ability of sago to grow well is due to sufficient water from rainfall to meet the water needs of sago plants (Yumna et al., 2020). In addition, the fibrous root system in sago and stem morphology with many xylem arrangements and growing in clusters can absorb more water (Azhar et al., 2021). This can reduce runoff water and prevent peak discharge and flooding.

The selection of sago plants as an alternative for water conservation in the upstream watershed and considering the suitability of the place to grow are also socio-economic factors (Metaragakusuma et al., 2017). The Rongkong watershed community still relies on sago products (sago starch) as a staple food and is designated as a regional mainstay commodity. Although the age of sago harvest is very long (10-14 years), it is possible to apply it with an agroforestry pattern to meet the needs and support the community's economy (Desmiwati et al., 2021). The extensification of sago to the upper watershed is very reasonable, both from the socio-economic aspect, especially in the ecological aspect, namely the flood disaster mitigation strategy in the middle and downstream parts. The age variability of sago growth is important because it is related to the plant canopy area that can capture and absorb rainwater (Yan et al., 2021).

This study aimed to measure changes in peak discharge in the upstream Rongkong watershed after experiencing changes in a sago-based land cover.

Materials and Methods

Study area

The research location is in the Rongkong watershed, South Sulawesi, Indonesia. Geographically, the Rongkong watershed is located at coordinates 2º 43' 37".8 - 3º 49 34.8 South Latitudes and 119º14' 49".7 - 120º 30' 0" East Longitude with an area of 190,748 ha. Rongkong watershed consists of two districts, distributed in nine sub-districts with details, North Luwu Regency includes seven sub-districts, namely Baebunta, Limbong, Malangke, West Malangke, Mappedeceng, Sabbang, and Seko sub-districts). Luwu Regency with two sub-districts (Lamasi and North Walenrang). The largest Rongkong watershed area is in Sabbang District, which occupies about 35.73% of the total area of the Rongkong watershed, then the second-largest is Limbong District (21.57%), then Lamasi District (12.36%), and the smallest area is in District North Walenrang is only 1.25% of the Rongkong watershed area. The slope varies from flat, sloping, wavy, and hilly to mountainous with slopes of 0-8%, 8-15%, 15-25%, 25-40%, and >40%. In the Rongkong watershed, around 64.40% (122,846 ha) of the area has a slope of >40% (Yumna et al., 2019).

This research consisted of two stages. The first stage was to measure the runoff coefficient for sago palms in three growth phases (initial, middle, and mature phases). The first stage was carried out in a demonstration plot/sago garden covering an area of 1 ha in West Malangke District, North Luwu Regency. The second stage of the research was to predict peak discharge for existing conditions and to simulate peak discharge based on several scenarios of changes in sago land cover in various growth phases. The location to be simulated was the upstream Salu Paku sub-watershed of the Rongkong watershed. The Salu Paku sub-watershed is the largest catchment area in the Rongkong watershed and contributes the most significant water discharge to the Rongkong river, resulting in flooding downstream. The map of the study area is presented in Figure 1.

Data collection

The data collected for this study consisted of primary and secondary data. Primary data included runoff data and rainfall data, which were measured directly on sago land, to determine the runoff coefficient of the sago palm.

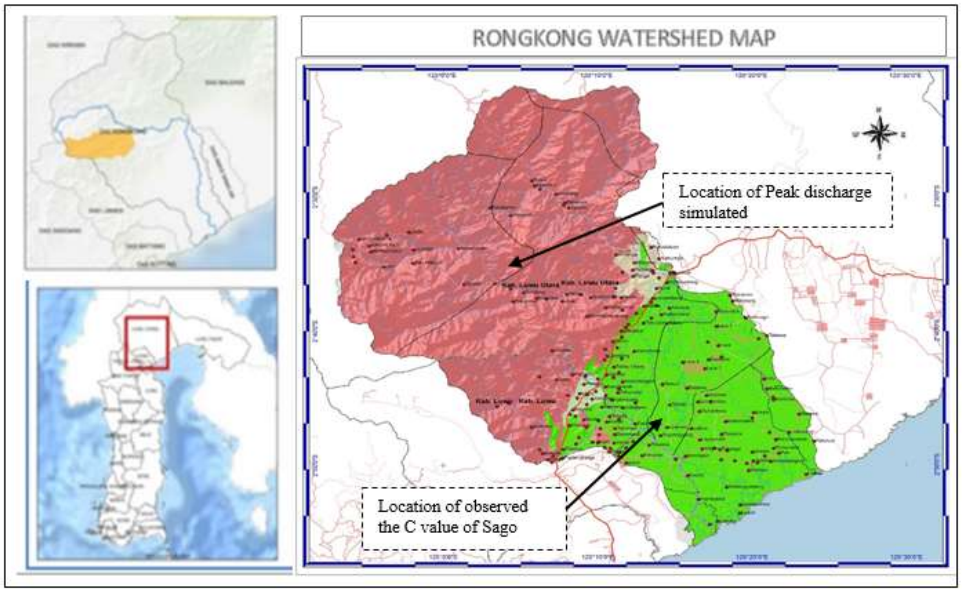

Figure 1. Study area in the Rongkong watershed, South Sulawesi, Indonesia.

Runoff was measured at three growth phases, i.e., initial phase (1-year-old plants), middle phase (5 years old plants), and mature phase (8 to 10 years old plants). Rainfall was measured using a simple Ombrometer with a diameter of 14 cm and a holding capacity of 3000 mL. Rainfall data had been calibrated with rainfall data from the Meteorology, Climatology, and Geophysics Agency of North Luwu Regency. Secondary data consisted of a land cover area in the existing conditions with reference to rational equations from the U.S. Forest Service 1980 (Asdak, 2018). The area of each simulation unit referred to the land cover condition resulting from the interpretation of the 30 m SRTM image from the USGS September 2018 coverage. It was validated directly in the field in 2020. Detailed data can be seen in Table 1.

Table 1. Land cover in the Salu Paku sub-watershed upstream of the Rongkong watershed.

Land Cover	Area (ha)	%
Settlement	2.227	0.02
Rice fields	29.909	0.22
Mixed gardens	92.049	0.68
Scrub	304.671	2.24
Sand dunes	14.155	0.10
Forest	13,120.075	96.29
Body of water/river	63.009	0.46
Total	**13,626.095**	**100**

Source: Yumna et al. (2019).

Data analysis

Runoff coefficient value (C)

The runoff coefficient is the ratio of runoff water (R) to rainfall (P) in the same period. This describes how much of the total rainwater turns into runoff. This formula has been widely used by previous researchers (Yan et al., 2021; Zheng et al., 2021; Bayad et al., 2022). The calculation formula is as follows:

$$C = R/P \quad \ldots\ldots\ldots\ldots\ldots\ldots\ldots\ldots\ldots\ldots\ldots\ldots\ldots (1)$$

where:

C = Runoff Coefficient
R = Runoff (mm)
P = Rainfall (mm)

The number of C ranges from 0 to 1. The number 0 (zero) indicates that all rainwater is distributed into interception and infiltration water; the number 1 (one) indicates that all rainwater flows as runoff. The runoff coefficient is generally greater than 0 and less than 1.

Peak discharge (Q)

The estimation of peak discharge in the upstream part of the Rongkong watershed was carried out after the data on the runoff coefficient and land area in each land unit were known. The existing peak discharge was estimated using the data from Table 1. The peak discharge for sago land was estimated based on three scenarios, namely 25% land unit area (Scenario 1), 50% land unit area (Scenario 2), and 100% land unit area (Scenario 3). The results of the estimation of existing conditions were compared with the results of the scenario. The scenario was determined based on the fact that there has been a gradual change in land cover. The scenario approach was also based on ease of analysis. This approach was performed by Dhofir and Choli (2018). The peak discharge (Q) was estimated using the rational method with the following equation:

$$Q = 0.0028\ C\ i\ A \quad \ldots\ldots\ldots\ldots \ (2)$$

where:

Q = Peak discharge (m^3 $second^{-1}$)
C = Runoff coefficient
i = highest rain intensity (mm $hour^{-1}$)
A = Watershed area/micro watershed (ha)

Comparison of peak discharge between existing land conditions and sago land scenarios

The scenarios used consisted of Scenario 1: 25% area of each land unit, Scenario 2: 50% area of each land unit, and Scenario 3: 100% of the area of each land unit. The land unit area was measured based on the upstream land cover of the Rongkong watershed (Salu Paku sub-watershed). The comparison of the existing peak discharge with the scenario results was made by quantitative description.

Results and Discussion

Runoff coefficient value (C)

The determination of the C value for sago land required rainfall and surface runoff data that were measured simultaneously at the same time and place. The runoff and rainfall data on the initial, middle and mature phases observation plots are presented in Figures 2, 3 and 4. The C value for the initial, middle and mature phases are presented in Figure 5, while the C value for the existing land cover can be seen in Table 2.

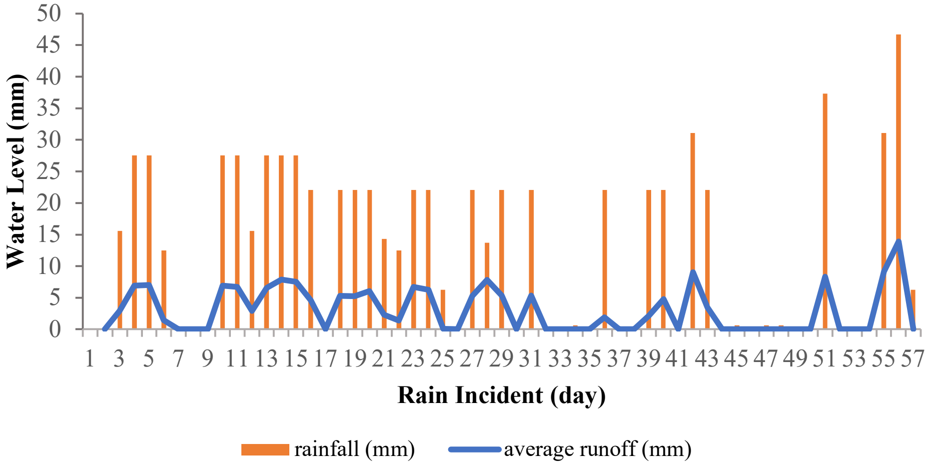

Figure 2. Rainfall and average runoff data within the day in the initial phase of sago plant growth.

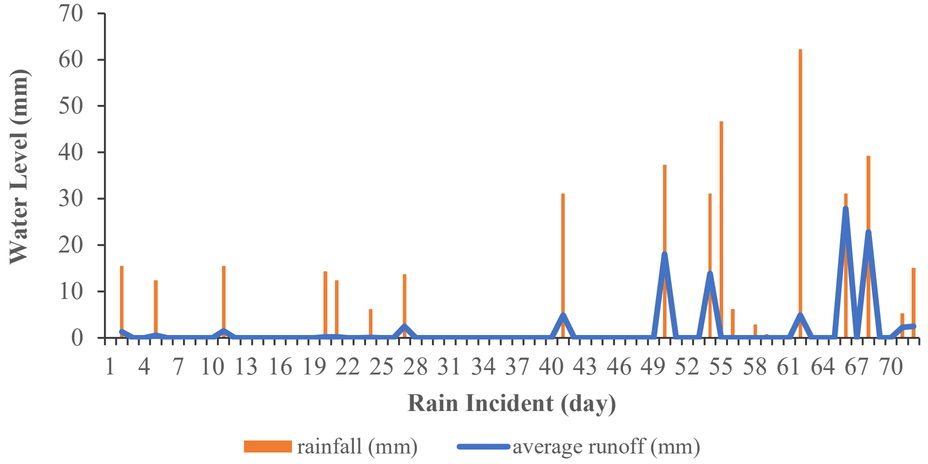

Figure 3. Rainfall and average runoff data within the day in the middle phase of sago plant growth.

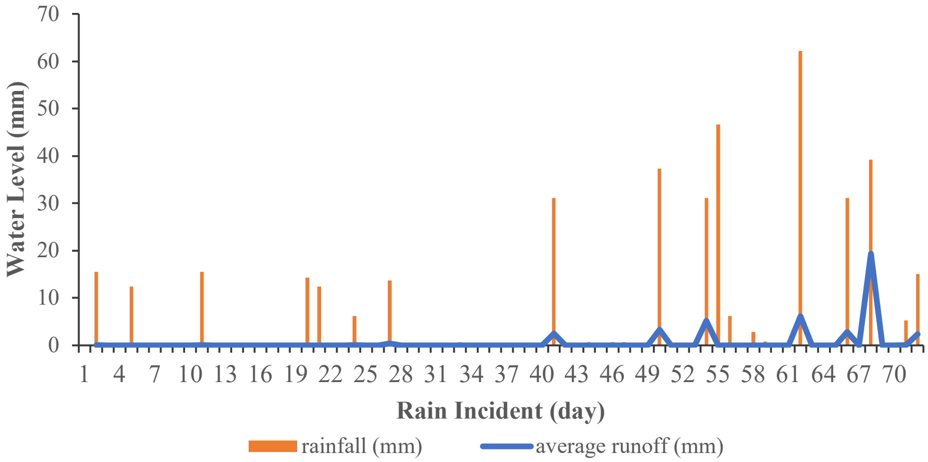

Figure 4. Rainfall and average runoff data within the day in the mature phase of sago plant growth.

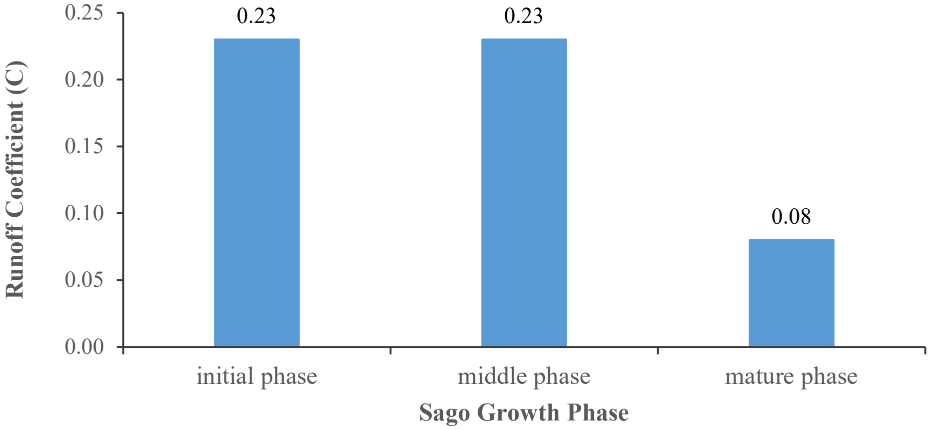

Figure 5. Runoff coefficient (C) for initial, middle, and mature phases in sago land.

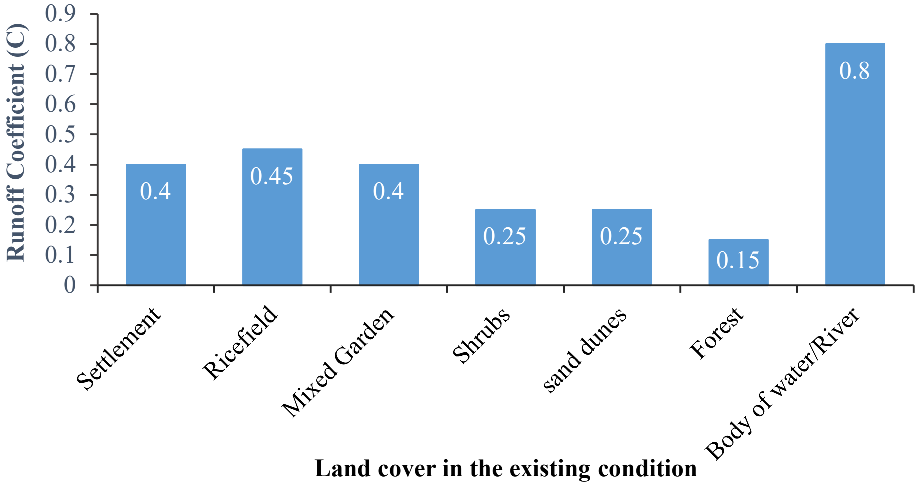

Figure 6. The runoff coefficient (C) for land cover in the existing conditions according to Asdak (2007).

Estimated peak discharge (Q)

The estimation results of peak discharge in existing conditions and after being simulated with changes in sago land used in several scenarios can be seen in Table 2. The results of the comparison between the existing conditions and the results of the scenarios are presented in Tables 3, 4 and 5. The ratio between runoff and rainfall in the three growth phases of the sago palm is shown in Figures 2, 3, and 4, so the runoff coefficient is presented in Figure 5. The C values in Figure 5 show that the initial and middle phases had the same value (0.23) and were higher than the mature phase (0.08). This value explains that about 23% of the rainwater turned into a runoff in the initial and middle phases of sago. While in the mature phase, it decreased to 8% of the total rainwater. The result of the direct measurement of the C value of sago land was different from the C value of land cover under the existing conditions (Figure 7).

Table 2. Estimated peak discharge under existing conditions and estimation results after being simulated with land-use changes for three-phase sago growth in three scenarios.

Land cover	**Q Existing (m^3 hour^{-1})**	**Q initial phase (m^3 hour^{-1})**			**Q middle phase (m^3 hour^{-1})**			**Q mature phase (m^3 hour^{-1})**		
		S3	**S2**	**S1**	**S3**	**S2**	**S1**	**S3**	**S2**	**S1**
Settlement	0.020	0.010	0.006	0.003	0.010	0.006	0.003	0.004	0.002	0.001
Rice fields	0.330	0.170	0.080	0.040	0.170	0.080	0.040	0.060	0.030	0.010
Mixed gardens	0.900	0.510	0.260	0.130	0.510	0.260	0.130	0.180	0.090	0.040
Scrub	1.860	1.690	0.850	0.420	1.700	0.850	0.430	0.590	0.290	0.140
Sand dunes	0.090	0.080	0.040	0.020	0.080	0.040	0.020	0.030	0.010	0.010
Forest	47.940	72.950	36.480	18.240	73.220	36.610	18.300	25.570	12.290	6.140
Body of water/river	1.230	0.350	0.180	0.090	0.350	0.180	0.090	0.120	0.060	0.030
Total	52.370	75.760	37.896	18.943	76.040	38.026	19.013	26.554	12.772	6.371

Remarks: S1 = Scenario 1, S2 = Scenario 2, S3 = Scenario 3.

Table 3. The comparison between the existing conditions with the results of the scenario in the initial phase.

Land cover	**Q existing (m^3 hour^{-1})**	**Q initial phase (m^3 hour^{-1})**			**Q difference result between**		
		S3	**S2**	**S1**	**Existing S3**	**Existing S2**	**Existing S1**
Settlement	0.020	0.010	0.006	0.003	0.010	0.014	0.017
Rice fields	0.330	0.170	0.080	0.040	0.160	0.250	0.290
Mixed gardens	0.900	0.510	0.260	0.130	0.390	0.640	0.770
Scrub	1.860	1.690	0.850	0.420	0.170	1.010	1.440
Sand dunes	0.090	0.080	0.040	0.020	0.010	0.050	0.070
Forest	47.940	72.950	36.480	18.240	-25.010	11.460	29.700
Body of water/river	1.230	0.350	0.180	0.090	0.880	1.050	1.140
Total	52.370	75.760	37.896	18.943	-23.390	14.474	33.427

Remarks: S1 = Scenario 1, S2 = Scenario 2, S3 = Scenario 3.

Table 4. The comparison between the existing conditions with the results of the scenario in the middle phase.

Land cover	**Q existing (m^3 hour^{-1})**	**Q middle phase (m^3 hour^{-1})**			**Q difference result between**		
		S3	**S2**	**S1**	**Existing S3**	**Existing S2**	**Existing S1**
Settlement	0.020	0.010	0.006	0.003	0.010	0.014	0.017
Rice fields	0.330	0.170	0.080	0.040	0.160	0.250	0.290
Mixed gardens	0.900	0.510	0.260	0.130	0.390	0.640	0.770
Scrub	1.860	1.700	0.850	0.430	0.160	1.010	1.430
Sand dunes	0.090	0.080	0.040	0.020	0.010	0.050	0.070
Forest	47.940	73.220	36.610	18.300	-25.280	11.330	29.640
Body of water/river	1.230	0.350	0.180	0.090	0.880	1.050	1.140
Total	52.370	76.040	38.026	19.013	-23.670	14.344	33.357

Remarks: S1 = Scenario 1, S2 = Scenario 2, S3 = Scenario 3.

Table 5. The comparison between the existing conditions with the results of the scenario in the mature phase.

Land cover	**Q existing** (m^3 hour^{-1})	**Q mature phase** (m^3 hour^{-1})			**Q difference result between**		
		S3	**S2**	**S1**	**Existing S3**	**Existing S2**	**Existing S1**
Settlement	0.020	0.004	0.002	0.001	0.016	0.018	0.019
Rice fields	0.330	0.060	0.030	0.010	0.270	0.300	0.320
Mixed gardens	0.900	0.180	0.090	0.040	0.720	0.810	0.860
Scrub	1.860	0.590	0.290	0.140	1.270	1.570	1.720
Sand dunes	0.090	0.030	0.010	0.010	0.060	0.080	0.080
Forest	47.940	25.570	12.290	6.140	22.370	35.650	41.800
Body of water/river	1.230	0.120	0.060	0.030	1.110	1.170	1.200
Total	52.370	26.554	12.772	6.371	25.816	39.598	45.999

Remarks: S1 = Scenario 1, S2 = Scenario 2, S3 = Scenario 3.

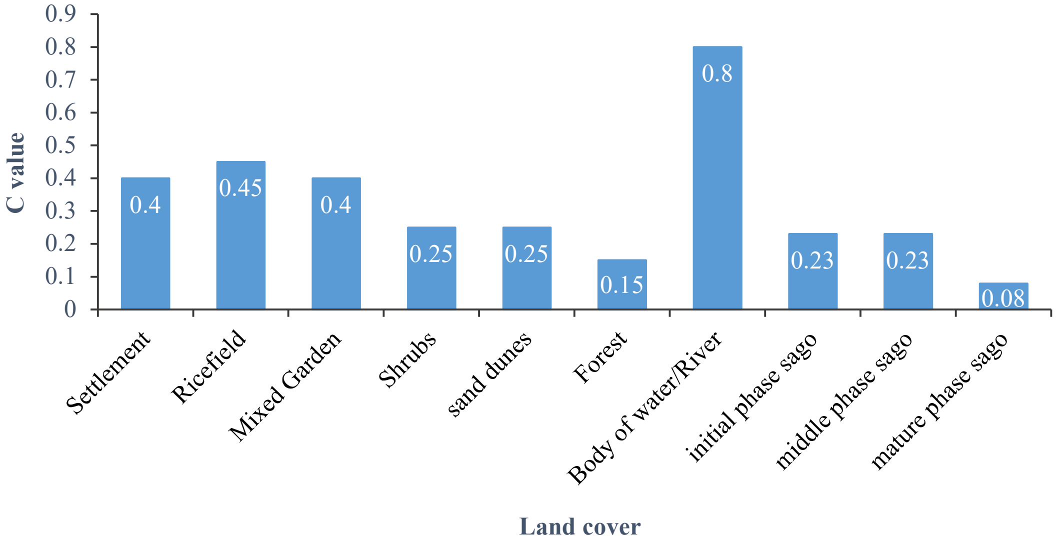

Figure 7. The comparison of the C value of existing land cover with sago land in three growth phases.

Figure 7 shows that the highest C value was found in the body of water/river land cover (0.8). This means that about 80% of the rainwater became runoff. The lowest C value was found in forest land cover (0.15), or only 15% of the rainwater that falls on forest areas turned into a runoff. However, after simulating the C value in the mature phase of sago land, it was still lower than the forest, namely 0.08 (8% of rainwater turned into runoff). Birch et al. (2021) and Chen et al. (2021) have proven the low runoff in the forest. Likewise, the body of water has the highest C value because all rainwater that falls in the area, especially rivers, will all become runoff and immediately flow to the lower part (downstream) (Ndehedehe et al., 2021). The C value from direct observation under sago stands at three growth phases showed a lower value than all land cover except forest. However, special in the mature phase, the value of C was still lower than in the forest. This means that the runoff product was lower under mature sago stands compared to forest. This condition is probably caused by the tight canopy cover of mature sago palms, and there is no gap for sunlight to enter the sago tree floor. This is evidenced by the high humidity under mature sago stands (Nelsi et al., 2021) and the high soil moisture content as a result of the infiltration and percolation processes of the sago root system (Yumna et al., 2020). The value of C then affects the magnitude of the peak discharge (Q) and the potential for flooding (Prokešová et al., 2022). Peak discharge estimated under two conditions, namely the existing condition and the condition after a change in sago-based land cover, is presented in Table 2. The magnitude of the estimated Q value was caused by land cover conditions and was influenced by the area of each land unit (Table 1). In the existing conditions, the value of Q on forest land cover is very large (47.94 mm^3 hour^{-1}) because the forest has the largest area in the study area, which is 96.29% of the total area of the study area, even though it has the lowest C value (0.15). When compared with the land cover that has the smallest peak discharge, namely settlements, the forest needs management attention so as not to worsen runoff water products (Lallemant et al., 2021). Based on Table 2, the total Q in the existing condition (52.37 m^3 hour^{-1}) and compared to the total Q from the scenario results, it can be seen that the existing condition has a lower peak discharge than the initial 3-phase scenario (75.76 mm^3 hour^{-1}) and the middle 3 phase scenario (76.04 mm^3 hour^{-1}). However, they were higher than scenarios 1 and 2 for the initial phase, scenarios 1, 2, and 3 for the middle phase, and scenarios 1, 2, and 3 for the mature phase. The higher peak discharge in scenario 3 for the initial phase than that of scenario 3 for the middle phase because in that scenario, the land was still in an open state (the canopy was not yet dense). By observing the conditions in scenario 3 in the initial and middle phases, it is highly recommended not to apply it, especially to forest land cover. Tables 3, 4, and 5 explain the ideal scenario based on the comparison results with the existing conditions. Scenarios that allow lowering the runoff can be seen in Figure 8. The initial phase of scenario 3 in Figure 8 explains that if there is a change in the sago land cover in the sapling phase (initial), covering an area of 100% of the existing condition area, there will be an increase in peak discharge by 23.39 mm^3 hour^{-1}. Likewise, with scenario 3 in the middle phase, if there is a change in land cover to sago saplings as large as the existing condition (100%), there will be an increase in peak discharge by 23.67 mm^3 hour^{-1}. In contrast to other scenarios, scenario 3 has the potential to reduce peak discharge.

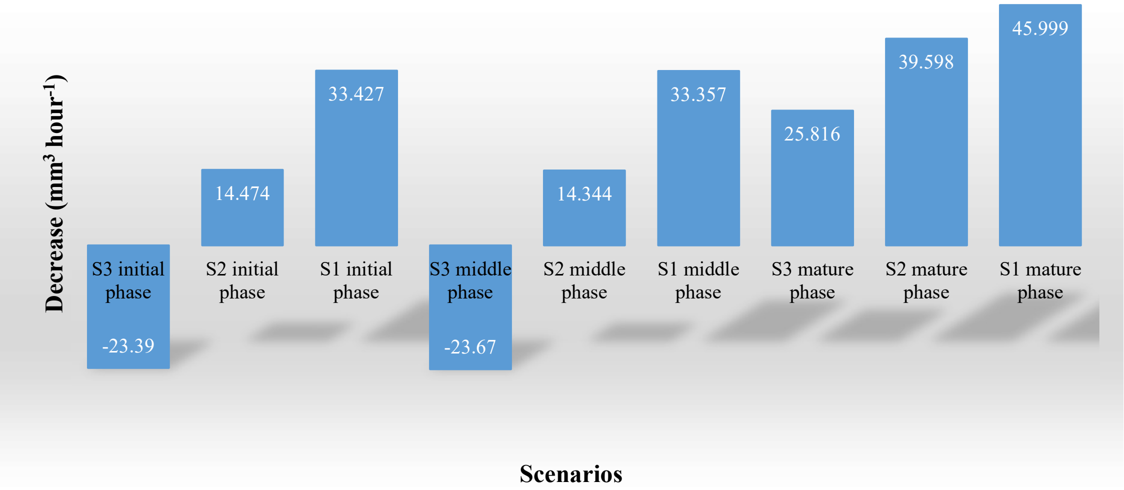

Figure 8. The potential of sago to reduce runoff based on the land cover change scenario.

The largest decrease in peak discharge occurred in scenario 1 of the mature phase, which changed 25% of the land area of the existing condition. Scenarios that are safe to apply to reduce peak discharge are scenario 1 of the initial phase (25% area), scenario 1 of the middle phase (25%), scenario 2 of the mature phase (50% area), and scenario 1 of the mature phase (25% area). However, because the age of sago growth to reach maturity is long (7 to 8 years), it is better not to change the land cover to sago palm simultaneously. The potential for sago to reduce runoff is caused by the morphology of sago starting from the canopy, stems, and roots which are ideal for absorbing and storing water (Marianus et al., 2012; Silangen, 2020).

Conclusion

The peak discharge changed with land cover change to sago land. The estimated peak discharge in the sago land cover scenario showed that the peak discharge tended to decrease except in the scenario of a 100% change in sago land cover in the initial and middle phases. A safe scenario is to change 25% of the existing land cover area. Although all scenarios in the mature phase are safe to apply, it must be taken into account that the age for sago palms is very long. So it is recommended to use a scenario of 25% of the total area for all land cover conditions, including changes in the land cover of forests.

Acknowledgements

This paper is part of a research conducted with support from Andi Djemma University. The authors thank the Chancellor of the Andi Djemma University and colleagues involved in this research.

References

Aburas, M.M., Ahamad, M.S.S. and Omar, N.Q. 2019. Spatio-temporal simulation and prediction of land-use change using conventional and machine learning models: a review. *Environmental Monitoring and*

Assessment 191(4):1-28, doi:10.1007/s10661-019-7330-6.

Ao, C., Zeng, W., Yang, P., Xing, W., Lei, G., Wu, J. and Huang, J. 2021. The effects of slope shape and polyacrylamide application on runoff, erosion and nutrient loss from hillslopes under simulated rainfall. *Hydrological Processes* 35(4):e14130, doi:10.1002/hyp.14130.

Asdak, C. 2007. *Hydrology and Watershed Management*. Gadjah Mada University Press.

Asitatikie, A.N., Kifelew, M.S. and Shumey, E.E. 2021. Flood inundation modeling using HEC-RAS: the case of downstream Gumara river, Lake Tana Sub Basin, Ethiopia. *Geocarto International* 1-10, doi:10.1080/10106049.2021.2022014.

Assefa, F., Elias, E., Soromessa, T. and Ayele, G.T. 2020. Effect of changes in land-use management practices on soil physicochemical properties in Kabe Watershed, Ethiopia. *Air, Soil and Water Research* 13, doi:10.1177/1178622120939587.

Azhar, A., Makihara, D., Naito, H., Asano, K., Takagi, M., Unoki, S., Tomita, R., Abbas, N. and Ehara, H. 2021. Sago palm (*Metroxylon sagu* Rottb.) response to drought conditions in terms of leaf gas exchange and chlorophyll a fluorescence. *Plant Production Science* 24(1):65-72, doi:10.1080/1343943X.2020.1794914.

Bayad, M., Chau, H.W., Trolove, S., Moir, J., Condron, L. and El Gharous, M. 2022. Surface runoff and losses of phosphorus from hydrophobic pastoral soils. *Agriculture, Ecosystems & Environment* 324:107690, doi:10.1016/j.agee.2021.107690.

Birch, A.L., Stallard, R.F., Bush, S.A. and Barnard, H.R. 2021. The influence of land cover and storm magnitude on hydrologic flow path activation and runoff generation in steep tropical catchments of central Panama. *Journal of Hydrology* 596:126138, doi:10.1016/j.jhydrol.2021.126138.

Chen, J., Li, Z., Xiao, H., Ning, K. and Tang, C. 2021. Effects of land use and land cover on soil erosion control in southern China: Implications from a systematic quantitative review. *Journal of Environmental Management* 282, doi:10.1016/j.jenvman.2020.111924.

de Almeida, W.S., Seitz, S., de Oliveira, L.F.C. and de Carvalho, D.F. 2021. Duration and intensity of rainfall events with the same erosivity change sediment yield and runoff rates. *International Soil and Water Conservation Research* 9(1):69-75, doi:10.1016/j.iswcr.2020.10.004.

Desmiwati, D., Veriasa, T.O., Aminah, A., Safitri, A.D., Wisudayati, T.A., Hendarto, K.A., Wisudayati, T.A., Royani, H., Dewi, K.H., Nur, S., Raharjo, I. and Sari, D.R. 2021. Contribution of agroforestry systems to farmer income in state forest areas: A case study of Parungpanjang, Indonesia. *Forest and Society* 109-119, doi:10.24259/fs.v5i1.11223.

Dhofir, Y.P. and Cholil, M. 2018. Analysis of Flood Potential Reduction from Hydrological Aspect through Spatial Modeling of Land Use Scenarios in the Upper Ciliwung Sub-Watershed, West Java. (*in Indonesian*).

Lallemant, D., Hamel, P., Balbi, M., Lim, T. N., Schmitt, R. and Win, S. 2021. Nature-based solutions for flood risk reduction: a probabilistic modeling framework. *One Earth 4*(9):1310-1321, doi:10.1016/j.oneear.2021.08.010.

Ma, M., Zhao, G., He, B., Li, Q., Dong, H., Wang, S. and Wang, Z. 2021. XGBoost-based method for flash flood risk assessment. *Journal of Hydrology* 598:126382, doi:10.1016/j.jhydrol.2021.126382.

Marianus, M., Ashari, S., Rahardjo, B.T. and Polii-Mandang, B. 2012. Sago baruk palm (*Arenga microcarpha* Becc) as a superior local food source and soil conservation plant at Sangihe Island Regency. *AGRIVITA, Journal of Agricultural Science* 34(2):144-151.

Metaragakusuma, A.P., Osozawa, K. and Hu, B. 2017. The current status of sago production in South Sulawesi: Its market and challenge as a new food-industry source. *International Journal Sustainable Future for Human Security J-SustaiN* 5(1):32-46.

Ming, R.Y. C., Sobeng, Y., Zaini, F. and Busri, N. 2018. Suitability of peat swamp areas for commercial production of sago palms: the Sarawak experience. *Sago Palm* 91-108.

Mu, X.M., Gu, C.J., Sun, W.Y., Zhao, G.J., Gao, P. and Wang, S.Y. 2019. Preliminary assessment effect of vegetation restoration on runoff generation pattern of the Loess Plateau. *Yellow River* 41(10):33-41.

Ndehedehe, C.E., Onojeghuo, A.O., Stewart-Koster, B., Bunn, S.E. and Ferreira, V.G. 2021. Upstream flows drive the productivity of floodplain ecosystems in tropical Queensland. *Ecological Indicators* 125:107546, doi:10.1016/j.ecolind.2021.107546.

Nelsi, O., Arsyad, U., Bachtiar, B. and Rampisela, D.A. 2021. Soil properties and infiltration rate in sago palm (Metroxylon sago) forest in Rongkong Watershed South Sulawesi. *IOP Conference Series: Earth and Environmental Science* 807(3):032053.

Prokešová, R., Horáčková, Š. and Snopková, Z. 2022. Surface runoff response to long-term land use changes: Spatial rearrangement of runoff-generating areas reveals a shift in flash flood drivers. *Science of the Total Environment* 815, doi:10.1016/j.scitotenv.2021.151591.

Ridwan, W.M., Sapitang, M., Aziz, A., Kushiar, K.F., Ahmed, A.N. and El-Shafie, A. 2021. Rainfall forecasting model using machine learning methods: Case study Terengganu, Malaysia. *Ain Shams Engineering Journal* 12(2):1651-1663, doi:10.1016/j.asej.2020.09.011.

Silangen, P.M. 2020. The analysis of ecological functions of sago baruk (*Arenga microcarpha* Becc) plants for sustainable use. *International Journal of Conservation Science* 11(3):791-798.

Sonu, T.S. and Bhagyanathan, A. 2022. The impact of upstream land use land cover change on downstream flooding: a case of Kuttanad and Meenachil River Basin, Kerala, India. *Urban Climate* 41:101089, doi:10.1016/j.uclim.2022.101089.

Sun, G., Gao, H. and Hao, L. 2021. Comments on large-scale afforestation significantly increases permanent surface water in China's vegetation restoration regions. *Agricultural and Forest Meteorology* 296:108213, doi:10.1016/j.agrformet.2020.108213.

Xu, G., Zhang, J., Li, P., Li, Z., Lu, K., Wang, X., Wang, F., Cheng, Y. and Wang, B. 2018. Vegetation restoration projects and their influence on runoff and sediment in China. *Ecological Indicators* 95:233-241, doi:10.1016/j.ecolind.2018.07.047.

Yan, L., Xue, L., Petropoulos, E., Qian, C., Hou, P., Xu, D. and Yang, L. 2021. Nutrient loss by runoff from rice-wheat rotation during the wheat season is dictated by rainfall duration. *Environmental Pollution* 285:117382, doi:10.1016/j.envpol.2021.117382.

Yan, T., Wang, Z., Liao, C., Xu, W. and Wan, L. 2021. Effects of the morphological characteristics of plants on rainfall interception and kinetic energy. *Journal of Hydrology* 592, doi:10.1016/j.jhydrol.2020.125807.

Yater, T., Tubur, H.W., Meliala, C. and Abbas, B. 2019. A comparative study of phenotypes and starch production in sago palm (Metroxylon sagu) growing naturally in temporarily inundated and non-inundated areas of South Sorong, Indonesia. *Biodiversitas Journal of Biological Diversity* 20(4):1121-1126, doi:10.13057/ biodiv/d200425.

Yumna, Prijono, S., Kusuma, Z. and Soemarno. 2019. Land suitability based on specific locations for sago palm (*Metroxylon sp.*) in rainfed drylands in the Salu Paku sub-watershed, the Rongkong upstream watershed, North Luwu Regency of South Sulawesi, Indonesia. *Russian Journal of Agricultural and Socio-Economic Sciences* 10(94):7-10, doi:10.18551/rjoas.2019-10.02.

Yumna, Y., Prijono, S., Kusuma, Z. and Soemarno, S. 2020. Community perception of rainfed sago land water management in Salu Paku Sub-watershed of Rongkong Watershed. *Jurnal Penelitian Kehutanan BONITA* 2(2):19-28 (*in Indonesian*).

Zheng, H., Miao, C., Zhang, G., Li, X., Wang, S., Wu, J. and Gou, J. 2021. Is the runoff coefficient increasing or decreasing after ecological restoration on China's Loess Plateau?. *International Soil and Water Conservation Research* 9(3):333-343, doi:10.1016/ j.iswcr.2021.04.009.